Spin-polarized β-stable neutron star matter: The nuclear symmetry energy and GW170817 constraint

Ngo Hai Tan [1,2,*] Dao T. Khoa [3] and Doan Thi Loan [3]

[1] *Faculty of Fundamental Sciences, Phenikaa University, Hanoi 12116, Vietnam*

[2] *Phenikaa Institute for Advanced Study (PIAS), Phenikaa University, Hanoi 12116, Vietnam*

[3] *Institute for Nuclear Science and Technology, VINATOM, 179 Hoang Quoc Viet, Cau Giay, Hanoi 100000, Vietnam*

(Received 20 March 2020; revised 27 July 2020; accepted 29 September 2020; published 19 October 2020)

The magnetic field of a rotating pulsar might be so strong that the equation of state (EOS) of neutron star (NS) matter is significantly affected by the spin polarization of baryons. In the present work, the EOS of the spin-polarized nuclear matter is investigated in the nonrelativistic Hartree-Fock formalism, using a realistic density-dependent nucleon-nucleon interaction with its spin- and spin-isospin dependence accurately adjusted to the Brueckner-Hartree-Fock results for spin-polarized nuclear matter. The nuclear symmetry energy and proton fraction are found to increase significantly with increasing spin polarization of baryons, leading to a larger probability of the direct Urca process in the cooling of magnetar. The EOS of the β-stable npeμ matter obtained at different spin polarizations of baryons is used as the input for the Tolman-Oppenheimer-Volkoff equations to determine the hydrostatic configuration of NS. Based on the GW170817 constraint on the radius $R_{1.4}$ of NS with $M \approx 1.4\,M_{\odot}$, our mean-field results show that up to 60% of baryons in the NS merger might be spin-polarized. This result supports the magnetar origin of the "blue" kilonova ejecta of GW170817 suggested by Metzger *et al.*, and the spin polarization of baryons needs, therefore, to be properly treated in the many-body calculation of the EOS of NS matter before comparing the calculated NS mass and radius with those constrained by the multimessenger GW170817 observation.

DOI: 10.1103/PhysRevC.102.045809

I. INTRODUCTION

Rotating pulsars are usually associated with strong magnetic field (B on the order of 10^{14} to 10^{19} G) [1–3], and effects of the magnetic field on the equation of state (EOS) of neutron star (NS) matter might not be negligible. This important issue has been investigated by many authors (see Sec. 9 of Ref. [1] and references therein), and the impact on the EOS by the magnetic field of a hydrodynamically stable NS was shown to be essential only if the field intensity $B \gtrsim 10^{18}$ G. In particular, the complete spin polarization of neutrons likely occurs at $B \gtrsim 4.41 \times 10^{18}$ G [2]. Given a common belief that the magnetic field of NS is usually much weaker than the upper limit of $B \approx 10^{19}$ G, it is often neglected in numerous mean-field studies of the EOS of NS matter. With the first direct observation of the binary NS merger GW170817 by the LIGO and Virgo Scientific Collaborations [4], a constraint on the tidal deformability of NS has been deduced and translated into a constraint on the radius and mass of NS [5]. This GW170817 constraint is now widely used to validate the mass and radius of NS predicted by different models, which usually neglect the spin polarization of baryons.

Recently, the "blue" kilonova ejecta observed in the aftermath of the NS merger GW170817 [6,7] have been suggested by Metzger *et al.* [8] to be caused by both the γ decay of the r-process nuclei and magnetically accelerated wind from the strongly magnetized hypermassive NS remnant. A rapidly rotating hypermassive NS remnant having the magnetic field of $B \approx (1\text{–}3) \times 10^{14}$ G at the surface was found necessary to explain the velocity, total mass, and enhanced electron fraction of the blue kilonova ejecta [8]. Because the strength of magnetic field remains quite strong in the outer core of magnetar [9], partial or full spin polarization of baryons might well occur during the GW170817 merger.

In general, the spin polarization of baryons can be explicitly taken into account in a microscopic model of nuclear matter (NM) with proper treatment of the spin- and spin-isospin dependencies of the in-medium interaction between baryons. For example, Vidaña *et al.* [10,11] have studied the spin-polarized neutron matter within the Brueckner-Hartree-Fock (BHF) formalism starting from a free nucleon-nucleon (NN) interaction, to explore the magnetic susceptibility of high-density neutron matter and possible phase transition to the ferromagnetic state as origin of the NS magnetic field. Aguirre *et al.* [12] have considered explicitly symmetric NM and neutron matter at finite temperature embedded in the external magnetic field with $B \simeq 10^{14}$–10^{18} G, and the spin polarization of baryons Δ was found strongest at low matter densities and becomes weaker with increasing baryon density $n_{\rm b}$. A similar study by Isayev and Yang [13] shows that high-density neutron matter embedded in the strong magnetic field might be partially spin-polarized when $B \gtrsim 10^{18}$ G. Tews and Schwenk have recently considered the EOS of fully

*tan.ngohai@phenikaa-uni.edu.vn

TABLE I. Yukawa strengths of the G-matrix based M3Y interaction [19].

ν	R_ν (fm^{-1})	$Y_{00}^{\rm D}(\nu)$ (MeV)	$Y_{10}^{\rm D}(\nu)$ (MeV)	$Y_{01}^{\rm D}(\nu)$ (MeV)	$Y_{11}^{\rm D}(\nu)$ (MeV)	$Y_{00}^{\rm EX}(\nu)$ (MeV)	$Y_{10}^{\rm EX}(\nu)$ (MeV)	$Y_{01}^{\rm EX}(\nu)$ (MeV)	$Y_{11}^{\rm EX}(\nu)$ (MeV)
1	4.0	11061.625	938.875	313.625	−969.125	−1524.25	−3492.75	−4118.0	−2210.0
2	2.5	−2537.5	−36.0	223.5	450.0	−518.75	795.25	1054.75	568.75
3	0.7072	0.0	0.0	0.0	3.4877	−7.8474	2.6157	2.6157	−0.8719

spin-polarized NS matter [14] and concluded that it is ruled out by the GW170817 constraint. The complex magnetic-field configuration of the magnetar has been investigated by Fujisawa and Kisaka [9], and the field intensity was shown to diminish gradually to $B \simeq 0$ from the surface to the center of the NS, so that the baryon matter in the center of the NS would not be spin-polarized even for magnetar. A partial spin polarization of NS matter is, however, not excluded by these studies, and it is of interest to investigate its impact on the EOS of NS matter.

Motivated by the magnetar scenario by Metzger *et al.* [8] for the "blue" kilonova ejecta of GW170817, we explore in the present work the EOS of the β-stable npeμ matter with different partial spin polarizations of baryons ($0 \lesssim \Delta \lesssim 1$). Like the isospin asymmetry, the spin asymmetry of baryons is shown to have a strong impact on the total energy and pressure of NM. In particular, the total nuclear symmetry energy has a strong repulsive contribution from the spin-symmetry energy, which in turn can affect significantly the radius and mass of a magnetar.

II. HARTREE-FOCK APPROACH TO THE SPIN-POLARIZED NUCLEAR MATTER

The nonrelativistic Hartree-Fock (HF) method [15] is used in the present work to study the spin-polarized NM at zero temperature, which is characterized by the neutron and proton number densities, $n_{\rm n}$ and $n_{\rm p}$, or equivalently by the total baryon number density $n_{\rm b} = n_{\rm n} + n_{\rm p}$ and neutron-proton asymmetry $\delta = (n_{\rm n} - n_{\rm p})/n_{\rm b}$. The spin polarization of baryons is treated explicitly for neutrons and protons by using the densities with baryon spin aligned up or down along the magnetic-field axis $\Delta_{\rm n,p} = (n_{\uparrow \rm n,p} - n_{\downarrow \rm n,p})/n_{\rm n,p}$. The total HF energy density of NM is obtained as

$$\mathcal{E} = \mathcal{E}_{\rm kin} + \frac{1}{2}\sum_{k\sigma\tau}\sum_{k'\sigma'\tau'}[\langle \boldsymbol{k}\sigma\tau, \boldsymbol{k}'\sigma'\tau'|v_{\rm D}|\boldsymbol{k}\sigma\tau, \boldsymbol{k}'\sigma'\tau'\rangle + \langle \boldsymbol{k}\sigma\tau, \boldsymbol{k}'\sigma'\tau'|v_{\rm EX}|\boldsymbol{k}'\sigma\tau, \boldsymbol{k}\sigma'\tau'\rangle], \quad (1)$$

where $|\boldsymbol{k}\sigma\tau\rangle$ are plane waves, and $v_{\rm D}$ and $v_{\rm EX}$ are the direct and exchange terms of the effective (in-medium) NN interaction.

We have considered for the present study the density-dependent CDM3Yn interaction that was successfully used in the HF studies of NM [15,16] and the folding model studies of nucleus-nucleus scattering [17,18]. In fact, the CDM3Yn interaction is the original G-matrix based M3Y interaction [19] supplemented by the realistic density dependencies $F_{\rm st}(n_{\rm b})$ of the spin- and spin-isospin-dependent terms of the M3Y interaction,

$$\begin{aligned} v_{\rm D(EX)}(n_{\rm b}, r) = {} & F_{00}(n_{\rm b})v_{00}^{\rm D(EX)}(r) + F_{10}(n_{\rm b})v_{10}^{\rm D(EX)}(r)(\boldsymbol{\sigma}\cdot\boldsymbol{\sigma}') \\ & + F_{01}(n_{\rm b})v_{01}^{\rm D(EX)}(r)(\boldsymbol{\tau}\cdot\boldsymbol{\tau}') \\ & + F_{11}(n_{\rm b})v_{11}^{\rm D(EX)}(r)(\boldsymbol{\sigma}\cdot\boldsymbol{\sigma}')(\boldsymbol{\tau}\cdot\boldsymbol{\tau}'). \end{aligned} \quad (2)$$

The radial parts of the direct and exchange terms of the interaction (2) are determined from the spin singlet and triplet components of the M3Y interaction [19] in terms of three Yukawa functions [20] (see Table I), $v_{\rm st}^{\rm D(EX)}(r) = \sum_{\nu=1}^{3} Y_{\rm st}^{\rm D(EX)}(\nu)\exp(-R_\nu r)/(R_\nu r)$.

Then the total-energy density (1) can be obtained as

$$\mathcal{E} = \frac{3}{10}\sum_{\sigma\tau}\frac{\hbar^2 k_{F\sigma\tau}^2}{m_\tau}n_{\sigma\tau} + F_{00}(n_{\rm b})\mathcal{E}_{00} + F_{10}(n_{\rm b})\mathcal{E}_{10} + F_{01}(n_{\rm b})\mathcal{E}_{01} + F_{11}(n_{\rm b})\mathcal{E}_{11}, \quad (3)$$

where $\sigma = \uparrow, \downarrow$ and $\tau = {\rm n}, {\rm p}$. The potential-energy density of NM is determined by using

$$\begin{aligned} \mathcal{E}_{00} &= \frac{1}{2}\left[n_{\rm b}^2 J_{00}^D + \int A_{00}^2 v_{00}^{\rm EX}(r)d^3r\right], \\ \mathcal{E}_{10} &= \frac{1}{2}\left[n_{\rm b}^2 J_{10}^D\left(\Delta_{\rm n}\frac{1+\delta}{2} + \Delta_{\rm p}\frac{1-\delta}{2}\right)^2 + \int A_{10}^2 v_{10}^{\rm EX}(r)d^3r\right], \\ \mathcal{E}_{01} &= \frac{1}{2}\left[n_{\rm b}^2 J_{01}^D\delta^2 + \int A_{01}^2 v_{01}^{\rm EX}(r)d^3r\right], \\ \mathcal{E}_{11} &= \frac{1}{2}\left[n_{\rm b}^2 J_{11}^D\left(\Delta_{\rm n}\frac{1+\delta}{2} - \Delta_{\rm p}\frac{1-\delta}{2}\right)^2 + \int A_{11}^2 v_{11}^{\rm EX}(r)d^3r\right]. \end{aligned} \quad (4)$$

$J_{\rm st}^D = \int v_{\rm st}(r)d^3r$ is the volume integral of the direct interaction, and the exchange integrals in Eq. (4) are evaluated with

$$\begin{aligned} A_{00} &= n_{\uparrow\rm n}\widehat{j}_1(k_{F_{\uparrow\rm n}}r) + n_{\downarrow\rm n}\widehat{j}_1(k_{F_{\downarrow\rm n}}r) + n_{\uparrow\rm p}\widehat{j}_1(k_{F_{\uparrow\rm p}}r) + n_{\downarrow\rm p}\widehat{j}_1(k_{F_{\downarrow\rm p}}r), \\ A_{10} &= n_{\uparrow\rm n}\widehat{j}_1(k_{F_{\uparrow\rm n}}r) - n_{\downarrow\rm n}\widehat{j}_1(k_{F_{\downarrow\rm n}}r) + n_{\uparrow\rm p}\widehat{j}_1(k_{F_{\uparrow\rm p}}r) - n_{\downarrow\rm p}\widehat{j}_1(k_{F_{\downarrow\rm p}}r), \\ A_{01} &= n_{\uparrow\rm n}\widehat{j}_1(k_{F_{\uparrow\rm n}}r) + n_{\downarrow\rm n}\widehat{j}_1(k_{F_{\downarrow\rm n}}r) - n_{\uparrow\rm p}\widehat{j}_1(k_{F_{\uparrow\rm p}}r) - n_{\downarrow\rm p}\widehat{j}_1(k_{F_{\downarrow\rm p}}r), \\ A_{11} &= n_{\uparrow\rm n}\widehat{j}_1(k_{F_{\uparrow\rm n}}r) - n_{\downarrow\rm n}\widehat{j}_1(k_{F_{\downarrow\rm n}}r) - n_{\uparrow\rm p}\widehat{j}_1(k_{F_{\uparrow\rm p}}r) + n_{\downarrow\rm p}\widehat{j}_1(k_{F_{\downarrow\rm p}}r), \end{aligned} \quad (5)$$

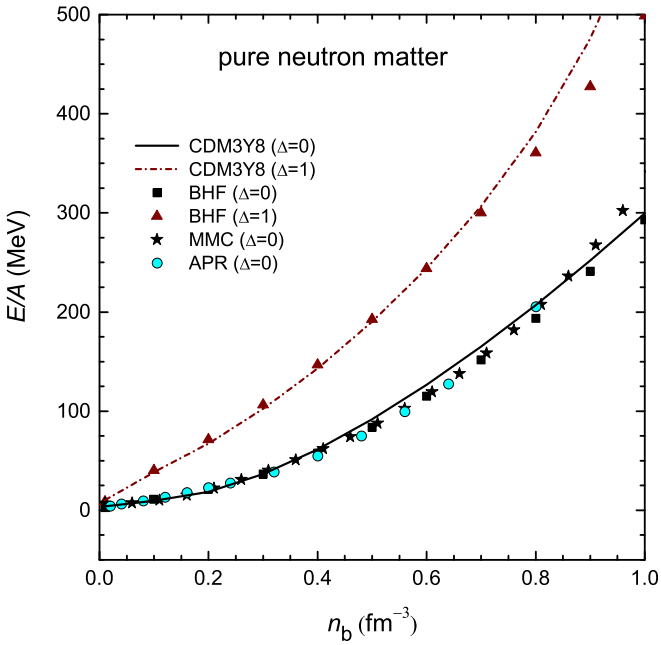

FIG. 1. Energy per baryon of pure neutron matter with the neutron spin polarization $\Delta = 0$ and 1 given by the HF calculation (5) using the newly parametrized CDM3Y8 interaction, in comparison with results of the BHF calculation (squares and triangles) [11]. The circles and stars are results of the *ab initio* calculations by Akmal, Pandharipande, and Ravenhall (APR) [21] and microscopic Monte Carlo (MMC) calculation by Gandolfi *et al.* [22], respectively.

where $\hat{j}_1(x) = 3j_1(x)/x$, and $j_1(x)$ is the first-order spherical Bessel function. The Fermi momentum of the spin-polarized baryon is determined as $k_{F\sigma\tau} = (6\pi^2 n_{\sigma\tau})^{1/3}$. One can see that the spin polarization of baryons gives rise to the nonzero contribution from both the $\mathcal{E}_{10}$ and $\mathcal{E}_{11}$ terms to the total NM energy density (3). Therefore, the density dependencies $F_{10}(n_b)$ and $F_{11}(n_b)$ of the CDM3Yn interaction (2) need to be properly determined for the present HF study. The spin-isospin independent (isoscalar) density dependence $F_{00}(n_b)$ was parametrized [17] to correctly reproduce the saturation properties of symmetric NM at the baryon density $n_0 \approx 0.16$ fm^{-3}, and the isospin dependent (isovector) density dependence $F_{01}(n_b)$ was adjusted to the BHF results of NM and fine tuned in the coupled-channel study of the charge exchange (p, n) reaction to isobar analog states in finite nuclei [23,24]. In the present work we have parametrized the density dependencies $F_{10}(n_b)$ and $F_{11}(n_b)$ of the spin- and spin-isospin-dependent parts of the CDM3Yn interaction in the same functional form as that used earlier for $F_{00}(n_b)$ and $F_{01}(n_b)$, and the parameters were adjusted to obtain the HF results for the spin-polarized neutron matter close to those of the BHF calculation by Vidaña *et al.* [11] using the Argonne V18 free NN potential added by the Urbana IX three-body force. The parameters of $F_{00}(n_b)$ and $F_{01}(n_b)$ were also slightly readjusted for a better agreement of the HF results with those of the *ab initio* calculations [21,22] at high baryon densities (see Fig. 1). This new version of the CDM3Yn interaction is referred to hereinafter as the CDM3Y8 interaction, with all parameters of the density dependence given explicitly in Table II.

TABLE II. Parameters of the density dependence of the CDM3Y8 interaction (2), $F_{st}(n_b) = C_{st}[1 + \alpha_{st}\exp(-\beta_{st}n_b) + \gamma_{st}n_b]$.

st	C_{st}	α_{st}	β_{st} (fm^3)	γ_{st} (fm^3)
00	0.2658	3.8033	1.4099	−4.300
01	0.2463	6.3836	10.2566	6.3549
10	0.2161	3.7510	−3.3396	9.9329
11	0.7572	1.9967	33.2012	0.2989

III. NUCLEAR SYMMETRY ENERGY

Although the neutron and proton magnetic moments are of different strengths and of opposite signs, in the presence of strong magnetic field $|\Delta_n|$ and $|\Delta_p|$ should be of the same order. We have assumed, for simplicity, the baryon spin polarization $\Delta = \Delta_n \approx -\Delta_p$ in the present HF study. The total NM energy per baryon E/A is then obtained in the *isospin* symmetry as

$$\frac{\mathcal{E}}{n_b} \equiv \frac{E}{A}(n_b,\ \Delta,\ \delta) = \frac{E}{A}(n_b,\ \Delta,\ \delta = 0) + S(n_b,\ \Delta)\delta^2 + O\left(\delta^4\right) + \cdots . \tag{6}$$

The contribution from $O(\delta^4)$ and higher-order terms in Eq. (6) is small and neglected in the *parabolic* approximation [20], where the isospin-symmetry energy $S(n_b, \Delta)$ equals the energy required per baryon to change symmetric NM into the pure neutron matter. Governed by the same SU(2) symmetry, such a parabolic approximation is also valid for the *spin* symmetry, and the total NM energy per baryon can be alternatively obtained as

$$\frac{\mathcal{E}}{n_b} \equiv \frac{E}{A}(n_b,\ \Delta,\ \delta) = \frac{E}{A}(n_b,\ \Delta = 0,\ \delta) + W(n_b,\ \delta)\Delta^2 + O\left(\Delta^4\right) + \cdots . \tag{7}$$

The exact spin-symmetry energy W given by the HF calculation (7) of symmetric NM and neutron matter are shown on the right panel of Fig. 2, and one can see that W is approximately Δ independent, and the contribution from $O(\Delta^4)$ and higher-order terms to the NM energy (7) is indeed negligible.

Given the quadratic dependence of the NM energy on the spin polarization of baryons and positive strength of the spin-symmetry energy W over the whole range of densities, it is sufficient to consider only $\Delta \geqslant 0$ in the present HF study. One can see in the left panel of Fig. 2 that the nonzero spin polarization significantly stiffens the EOS of NM. In particular, the symmetric NM becomes unbound by the strong interaction at $\Delta \gtrsim 0.75$ in about the same way as the asymmetric NM becomes unbound by the in-medium NN interaction with the increasing neutron-proton asymmetry $\delta \gtrsim 0.75$ [20].

The isospin-symmetry energy $S(n_b, \Delta)$, widely discussed in the literature as the *nuclear symmetry energy*, is a key characteristics of the EOS of neutron-rich NM. In particular, the knowledge about the density dependence of $S(n_b)$ is

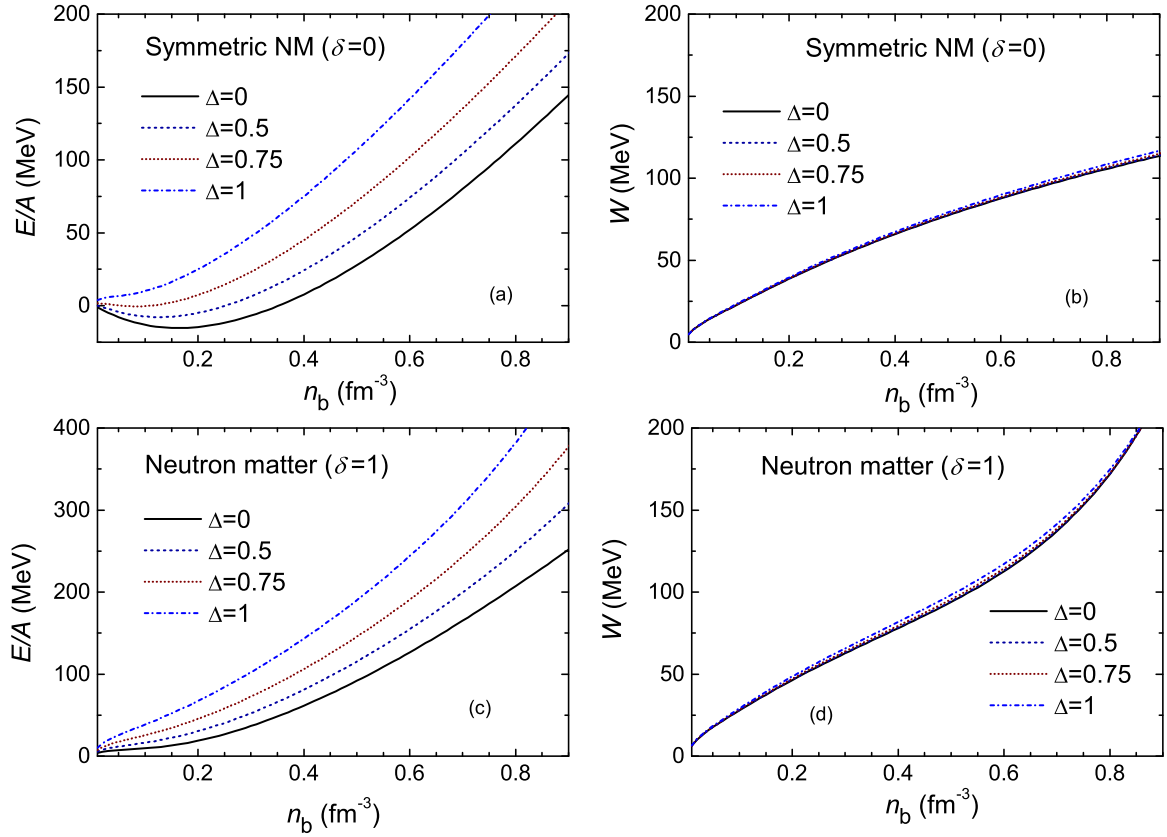

FIG. 2. The present HF results obtained at different spin polarizations Δ of baryons for the energy per baryon E/A and spin-symmetry energy W of symmetric NM, panels (a) and (b), respectively, and those of neutron matter, panels (c) and (d), respectively.

extremely important for the determination of the nuclear EOS and it has been, therefore, a longstanding goal of numerous nuclear physics and nuclear astrophysics studies (see, e.g., Refs. [30–32]). However, the results of these studies were mainly obtained for the spin-saturated NM, and describe, therefore, the behavior of $S(n_b, \Delta = 0)$.

The nuclear symmetry energy is rather well constrained at low baryon densities by the analyses of the (isospin dependent) data of heavy-ion (HI) collisions [25,26] as well as the structure studies of the giant dipole resonance [27] or neutron skin [28]. Our HF results for $S(n_b, \Delta)$ are compared with the empirical data in Fig. 3, and a significant increase of the nuclear symmetry energy is found with the increasing spin polarization of baryons Δ. At low densities, the calculated $S(n_b, \Delta)$ values fall within the empirical range when the baryon spin polarization $\Delta \lesssim 0.75$. The behavior of the nuclear symmetry energy at high baryon densities ($n_b > n_0$) remains not well determined. However, the mass and radius of NS (given, e.g., by the Tolman-Oppenheimer-Volkoff equations using different EOSs of NS matter) are proven to be strongly sensitive to the strength and slope of $S(n_b)$ at high densities [15,29]. Recently, Xie and Li [29] have inferred the symmetry energy at baryon densities up to $3n_0$ from a statistical Bayesian analysis of the correlation of different EOSs of the npeμ matter and associated radius $R_{1.4}$ of NS with mass $M \approx 1.4\ M_\odot$ versus the GW170817 constraint on $R_{1.4}$ imposed by the NS tidal deformability. In particular, the EOS with the symmetry energy at twice the saturation density $S(2n_0) \approx 40$–60 MeV give $R_{1.4}$ radii within the range constrained by the tidal deformability. The empirical $S(n_b)$ values suggested for baryon densities up to $3n_0$ at 90% confidence level [29] are shown in Fig. 3, and they cover the symmetry energy predicted by the HF calculation of neutron-rich NM over the whole range of the spin polarization of baryons $0 \lesssim \Delta \lesssim 1$. One can trace in Fig. 3 that the symmetry energy obtained with a narrower uncertainty (at 68% confidence level) $S(2n_0) \approx 39.2^{+12.1}_{-8.2}$ MeV [29] also covers all possible spin polarizations.

To explore the density dependence of the nuclear symmetry energy, S is often expanded around the saturation density n_0 [30–32] in terms of the symmetry coefficient J, slope L, and curvature $K_{\rm sym}$. With the spin polarization of baryons treated explicitly in the present HF study, these quantities are now dependent on the spin polarization Δ, and we obtain

$$S(n_b, \Delta) = J(\Delta) + \frac{L(\Delta)}{3}\left(\frac{n_b - n_0}{n_0}\right) + \frac{K_{\rm sym}(\Delta)}{18}\left(\frac{n_b - n_0}{n_0}\right)^2 + \cdots . \quad (8)$$

$J(\Delta)$, $L(\Delta)$, $K_{\rm sym}(\Delta)$, and the incompressibility $K_0(\Delta)$ of symmetric NM at the saturation density (which also depends on the spin polarization of baryons) are the most important characteristics of the EOS of the spin-polarized NM. The J, L, $K_{\rm sym}$, K_0 values given by the present HF calculation using the CDM3Y8 interaction are given in Table III.

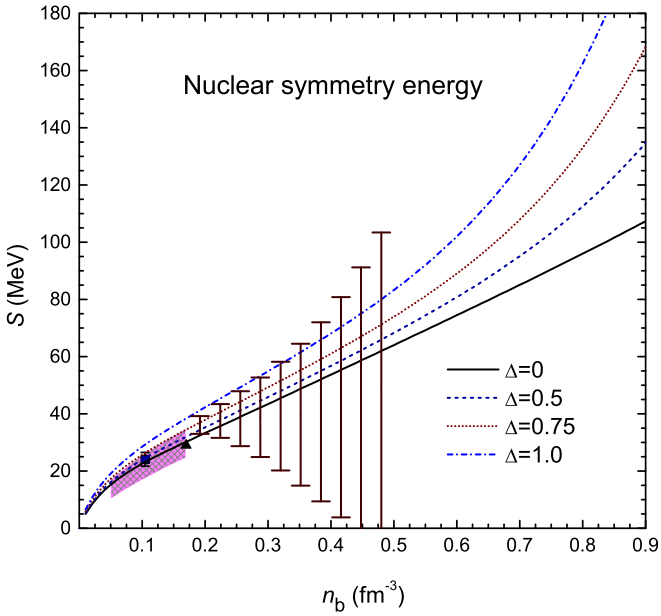

FIG. 3. The nuclear symmetry energy $S(n_b, \Delta)$ given by the HF calculation (6) assuming different spin polarizations of baryons Δ. The shaded region is the range constrained by the data of HI collisions [25,26]. The square and triangle are values suggested by the nuclear structure studies [27,28]. The vertical bars are the empirical range obtained at the 90% confidence level in a statistical Bayesian analysis [29] of the NS radius $R_{1.4}$ versus the GW170817 constraint [5].

Among these quantities, the incompressibility K_0 of symmetric NM has been the key research topic of numerous structure studies of nuclear monopole excitations (see, e.g., review [33] and references therein) as well as the studies of HI collisions and refractive nucleus-nucleus scattering [34]. These researches have pinned down this quantity to $K_0 \approx 240 \pm 20$ MeV. The symmetry coefficient and slope of the nuclear symmetry energy (8) were also extensively investigated and inferred independently from different analyses of terrestrial nuclear physics experiments and astrophysical observations, and they are now constrained to $J \approx 31.7 \pm 3.2$ MeV and $L \approx 58.7 \pm 28.1$ MeV [35]. The $K_{\rm sym}$ value is still not well determined and remains within a wide range $-400\ {\rm MeV} \lesssim K_{\rm sym} \lesssim 100$ MeV [35]. The HF results for J, L, $K_{\rm sym}$, and K_0 of the spin-saturated NM with $\Delta = 0$ agree well with the empirical values and remain within the empirical boundaries with the spin polarization of baryons $0 \lesssim \Delta \lesssim 0.8$.

TABLE III. The symmetry coefficient J, slope L, and curvature $K_{\rm sym}$ of the symmetry energy (8), and incompressibility K_0 of symmetric NM at the saturation density n_0 given by the HF calculation of the spin-polarized NM using the CDM3Y8 interaction.

Δ	J (MeV)	L (MeV)	$K_{\rm sym}$ (MeV)	K_0 (MeV)
0.0	29.5	50.6	−254	244
0.1	29.6	50.7	−256	243
0.2	29.8	51.0	−264	242
0.3	30.1	51.6	−275	240
0.4	30.6	52.5	−291	238
0.5	31.3	53.5	−314	234
0.6	32.1	54.9	−340	230
0.7	33.1	56.6	−369	225
0.8	34.3	58.7	−402	219
0.9	35.7	61.3	−450	213
1.0	37.5	64.7	−505	205

IV. BETA-STABLE NEUTRON-STAR MATTER

For the EOS of inhomogeneous NS crust, we have adopted that given by the nuclear energy-density functional (EDF) calculation [36,37] using the BSk24 Skyrme functional, with atoms being fully ionized and electrons forming a degenerate Fermi gas. At the edge density $n_{\rm edge} \approx 0.076$ fm^{-3}, a weak first-order phase transition takes place between the NS crust and uniform core of NS. At baryon densities $n_b \gtrsim n_{\rm edge}$ the NS core is described as a homogeneous matter of neutrons, protons, electrons, and negative muons (μ^- appear at n_b above the muon threshold density $\mu_e > m_\mu c^2 \approx 105.6$ MeV).

A. Density-independent spin polarization of the npeμ matter

To explore the impact of the spin polarization of baryons on the EOS of the β-stable npeμ matter of NS, we assumed for simplicity that the spin polarization of baryons Δ is density independent and varied Δ within the range $(0 \to 1)$ at each considered density, as done above for the spin-polarized NM. Then, the total-energy density $\mathcal{E}$ of the npeμ matter (including the rest energy) is determined as

$$\mathcal{E}(n_{\rm n}, n_{\rm p}, n_e, n_\mu, \Delta) = \mathcal{E}_{\rm HF}(n_{\rm n}, n_{\rm p}, \Delta) + n_{\rm n} m_{\rm n} c^2 + n_{\rm p} m_{\rm p} c^2 + \mathcal{E}_e(n_e) + \mathcal{E}_\mu(n_\mu), \quad (9)$$

where $\mathcal{E}_{\rm HF}(n_{\rm n}, n_{\rm p}, \Delta)$ is the HF energy density (3) of the spin-polarized NM, $\mathcal{E}_e$ and $\mathcal{E}_\mu$ are the energy densities of electrons and muons given by the relativistic Fermi gas model [38]. In such a Fermi gas model, the spin polarization of leptons does not affect the total energy density $\mathcal{E}$, and the lepton number densities n_e and n_μ can be determined from the charge neutrality condition ($n_{\rm p} = n_e + n_\mu$) and the β equilibrium of (neutrino-free) NS matter in the same way as done for the spin unpolarized NS matter (see Ref. [15] for more details).

The density-dependent proton fraction $x_{\rm p}(n_b)$ is a key input for the determination of the NS cooling rate. In particular, the direct Urca (DU) process of NS cooling via neutrino emission is possible only if the proton fraction is above the DU threshold $x_{\rm DU}$ [15]:

$$x_{\rm DU}(n_b) = \frac{1}{1 + \left[1 + r_e^{1/3}(n_b)\right]^3}, \quad (10)$$

where $r_e(n_b) = n_e/(n_e + n_\mu)$ is the leptonic electron fraction at the given baryon number density. At low densities $r_e = 1$ and $x_{\rm DU} \approx 11.1\%$, which corresponds to the muon-free threshold for the DU process. Because the lepton-baryon interaction is neglected in the present study, the $x_{\rm DU}$ value

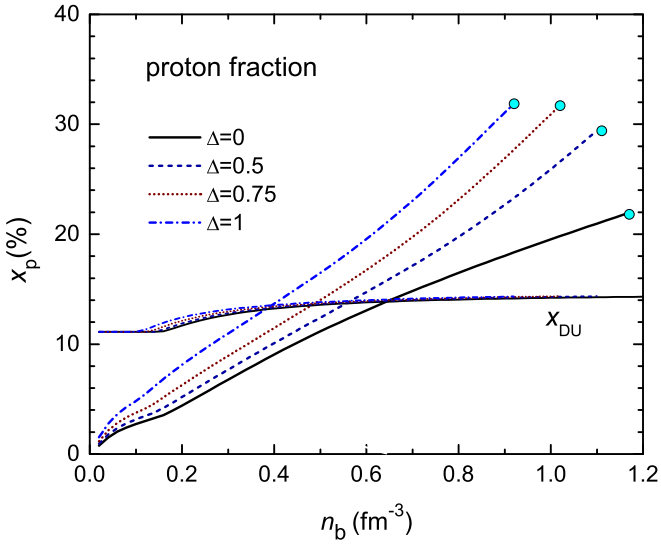

FIG. 4. The proton fraction x_p determined from the charge neutrality of the spin-polarized β-stable npeμ matter obtained with the HF energy density (3) using the CDM3Y8 interaction. The circles are n_p values calculated at the maximum central densities n_c, and the thin lines are the DU thresholds (10).

determined from the β-equilibrium condition depends very weakly on the spin-polarization of baryons. The proton fraction x_p of the spin-polarized β-stable npeμ matter obtained with the HF energy density (3) using the CDM3Y8 interaction is shown in Fig. 4, and one can see that x_p increases significantly with the increasing spin polarization of baryons, and it exceeds the DU threshold at densities $n_b \gtrsim 2n_0$ if baryons are completely spin polarized ($\Delta = 1$). From the behavior of n_p shown in Fig. 4 we find that the electron fraction in the β-stable npeμ matter also increases with the increasing Δ and might reach up to 20%–30% at high densities when Δ approaches 1. It is remarkable that such a high electron fraction was found in the blue kilonova ejecta following the NS merger GW170817 [6,7] and suggested by Metzger *et al.* [8] to be of the magnetar origin.

The mass density ρ and total pressure P of NS crust given by the EDF calculation at baryon densities below the edge density $n_{edge} \approx 0.076$ fm^{-3}, and those of the uniform and spin-polarized npeμ matter given by the HF calculation at $n_b \gtrsim n_{edge}$ have been used as inputs for the Tolman-Oppenheimer-Volkoff (TOV) equations to determine the hydrostatic configuration of NS (see Table IV). For a consistent mean-field study of the spin-polarized npeμ matter of NS, we have used in this work two versions of NS crust: the unmagnetized crust ($B_{crust} = 0$) and crust embedded in the magnetic field of $B_{crust} = 1.323 \times 10^{17}$ G [37]. The effects of magnetic field on the EOS and the composition of NS crust were shown mainly due to the Landau quantization of the electron motion, with most protons and neutrons remaining "packed" in nuclei with $Z \approx 40$–50 inside in the Wigner-Seitz cell [37]. The impact of the magnetic field with $B_{crust} \approx 10^{17}$ G is strong in the outer crust (see Fig. 5), while the EOS of the inner crust remains almost unchanged compared with that of the unmagnetized crust at baryon densities $n_b \gtrsim 0.01$ fm^{-3}.

TABLE IV. Configuration of NS given by the EOS of the spin-polarized β-stable npeμ matter obtained with the CDM3Y8 interaction. M_{max} and R_{max} are the maximal gravitational mass and radius; $R_{1.4}$, n_c, and P_c are the radius of the NS with $M \approx 1.4\,M_\odot$, central baryon number density, and central total pressure, respectively. $P(2n_0)$ is the total pressure at twice the saturation density.

Δ	M_{max} ($M_\odot$)	R_{max} (km)	$R_{1.4}$ (km)	n_c (fm^{-3})	P_c (10^{35} dyn/cm^2)	$P(2n_0)$ (10^{34} dyn/cm^2)
0.0	1.98	10.3	12.0	1.17	9.9	3.4
0.1	1.99	10.3	12.0	1.16	10.0	3.5
0.2	2.00	10.4	12.1	1.16	10.2	3.6
0.3	2.02	10.4	12.3	1.15	10.4	3.6
0.4	2.04	10.5	12.5	1.14	10.9	3.9
0.5	2.06	10.6	12.8	1.11	10.3	4.1
0.6	2.08	10.8	13.1	1.08	10.0	4.4
0.7	2.10	11.1	13.6	1.04	9.5	4.6
0.8	2.12	11.3	14.1	1.01	9.0	5.0
0.9	2.14	11.7	14.8	0.96	8.1	5.4
1.0	2.16	12.0	15.6	0.92	7.7	5.8

As a result, the main properties of NS shown in Table IV are not affected by the magnetization of the NS crust. We note that the spin polarization of free baryons and spin-unsaturated nuclei inside the Wigner-Seitz cell has not been taken into account in the EDF approach [37], and it might result in a stronger impact of the magnetic field on the EOS of the NS crust.

Because NS matter becomes less compressible (see K_0 values in Table III) when the spin polarization of baryons is nonzero, the central density n_c and pressure P_c decrease with increasing Δ. As a result, the NS expands its size and the maximal gravitational mass M_{max} and radius R_{max} become larger with increasing spin polarization of baryons. The LIGO and Virgo data of the NS merger GW170817 were analyzed by Abbott *et al.* [5] to put constraints on the tidal deformability of two merging neutron stars, which were then translated into constraints on NS radius. By requiring that a realistic

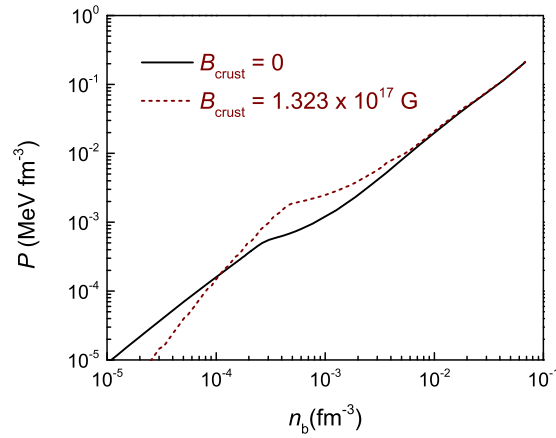

FIG. 5. Pressure P in the unmagnetized ($B_{crust} = 0$) and magnetized ($B_{crust} \neq 0$) crust of a NS given by the EDF calculation [36,37] using the BSk24 Skyrme functional.

EOS of NS matter must accommodate the NS maximal mass $M_{\rm max} \gtrsim 1.97\,M_\odot$, Abbott *et al.* have obtained the radius of a NS with $M \approx 1.4\,M_\odot$ in the range $R_{1.4} \approx 11.9 \pm 1.4$ km at the 90% confidence level [5]. This analysis has also given a constraint on the total pressure of NS matter at supra-saturation densities; namely, $P(2n_0) \approx 3.5^{+2.7}_{-1.7} \times 10^{34}$ dyn/cm^2 at the same 90% confidence level. One can see from NS properties given by the EOS of the spin-polarized β-stable npeμ matter shown in Table IV that the GW170817 constraints are fulfilled with the spin polarization of baryons $\Delta \lesssim 0.6$ for the $R_{1.4}$ radius and $\Delta \lesssim 1$ for the total pressure $P(2n_0)$ of NS matter, respectively. The NS maximal mass $M_{\rm max}$ obtained with the EOS given by the CDM3Y8 interaction increases from $1.98\,M_\odot$ to $2.16\,M_\odot$ with the spin polarization Δ increasing from 0 to 1. This range of the $M_{\rm max}$ values covers well the observed NS masses $M \approx (1.908 \pm 0.016)\,M_\odot$, $(2.01 \pm 0.04)\,M_\odot$, and $(2.14 \pm 0.09)\,M_\odot$ of the binary pulsars PSR J1614-2230 [39,40], PSR J0348+0432 [41], and PSR J0740+6620 [42], respectively. Note that the large NS mass $M \approx 2.14\,M_\odot$ seems possible in the present mean-field scenario only when baryons are completely spin polarized ($0.9 \lesssim \Delta \lesssim 1$).

The constraint on the radius $R_{1.4}$ of NS with $M \approx 1.4\,M_\odot$ deduced from the multimessenger observation of GW170817 [5] has now become an important reference for the mean-field studies or Bayesian analyses of the EOS of NS matter to narrow the uncertainty of the symmetry energy (8) at high baryon densities [29,43]. For example, Tsang *et al.* [43] have shown a systematic correlation of the J, L, and $K_{\rm sym}$ values with the tidal deformability of NS, using about 200 different sets of Skyrme interaction in their mean-field study. From the GW170817 constraint on the radius $R_{1.4}$ and tidal deformability, some correlation between the symmetry energy at high baryon densities and $R_{1.4}$ radius can be inferred. By comparing the J, L, and $K_{\rm sym}$ values given by our HF calculation of the spin-polarized NM shown in Table III and $R_{1.4}$ radii obtained at different Δ values shown in Table IV, we found that J, L, and $|K_{\rm sym}|$ are almost linearly correlated with the $R_{1.4}$ radius (see Fig. 6). In particular, with the increasing spin polarization of baryons, the larger the slope L of the symmetry energy, the larger the corresponding $R_{1.4}$ radius. One can see in Fig. 6 that the spin polarization of baryons is confined by the GW170817 constraint to the range $0 \lesssim \Delta \lesssim 0.6$, where 50.6 MeV $\lesssim L \lesssim$ 54.9 MeV and 12 km $\lesssim R_{1.4} \lesssim$ 13.1 km. From the correlation between L and $R_{1.4}$ shown in Fig. 6, it is not excluded that an EOS of the spin-unpolarized NS matter with $L \gtrsim 65$ MeV would give a radius $R_{1.4} > 13.1$ km.

Our results obtained for the correlation of the mass and radius of NS given by the EOS of β-stable spin-polarized npeμ matter with Δ increasing from 0 to 1 are shown in Fig. 7. The GW170817 constraint for the radius $R_{1.4}$ of NS with $M \approx 1.4\,M_\odot$ are plotted in Fig. 7 as the shaded contours. One can see that all mass-radius curves with $\Delta \lesssim 0.6$ go well through the GW170817 contours. The upper bound of 13.3 km for $R_{1.4}$ [5] is exceeded when more than 60% of baryons are spin polarized. Combined with the impact on the symmetry energy shown in Figs. 3 and 6, the upper limit of $\Delta \approx 0.6$ shown in Fig. 7 might well narrow the uncertainty

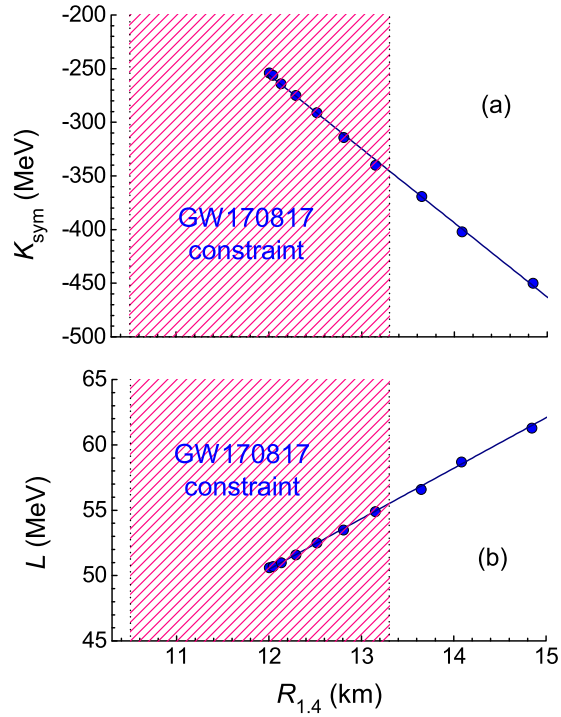

FIG. 6. The curvature $K_{\rm sym}$ and slope L of the nuclear symmetry energy (8) versus the radius $R_{1.4}$ of NS with $M \approx 1.4\,M_\odot$ shown as solid circles in panels (a) and (b), respectively, are given by the EOS of the spin-polarized β-stable npeμ matter with Δ increasing from 0 to 0.9 (see also Tables III and IV). The shaded areas enclose the range of the $R_{1.4}$ radius constrained by the tidal deformability of NS [5].

of the symmetry energy S, its slope L, and curvature $K_{\rm sym}$ at supra-saturation baryon densities ($n_{\rm b} > n_0$). As shown in Table IV and Fig. 7, the maximal gravitational mass $M_{\rm max}$ and radius $R_{\rm max}$ of NS in the hydrostatic equilibrium can be strongly affected by the spin polarization of baryons. We note that all the calculated $M_{\rm max}$ values are above the lower limit of $1.97\,M_\odot$ that was imposed on the GW170817 constraint for the $R_{1.4}$ radius by Abbott *et al.* [5]. The results shown in the upper and lower panels of Fig. 7 confirm that the effect of the magnetization of the NS crust [37] on the NS mass and radius is negligible. It remains uncertain if this conclusion still holds when the spin polarization of free baryons as well as the spin-unsaturated nuclei in the Wigner-Seitz cell in the NS crust is treated explicitly.

In conclusion, the present mean-field study shows that the spin polarization of baryons affects strongly the EOS of the NS matter via the spin- and spin-isospin-dependent channels of the in-medium interaction between baryons. In particular, the symmetry energy of the spin-polarized NM (with $\Delta \neq 0$) was found to be much stiffer at high baryon densities compared with that of the spin-saturated NM (with $\Delta = 0$), and this can affect significantly the hydrostatic configuration of NS. Based on the GW170817 constraint for the $R_{1.4}$ radius [5], baryons in the two merging neutron stars could be partially spin-polarized with $0 \lesssim \Delta \lesssim 0.6$ (see Fig. 7). We found, however, that the GW170817 constraint excludes the full spin polarization of baryons in NS matter ($\Delta = 1$), and

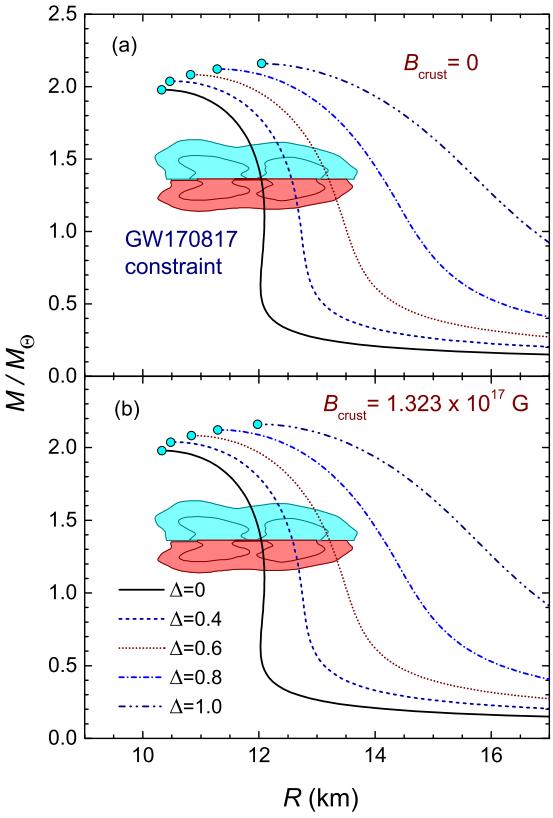

FIG. 7. Correlation of the mass and radius of NS given by the EOS of β-stable spin-polarized npeμ matter ($\Delta = 0 \rightarrow 1$) obtained with the CDM3Y8 interaction (2). The results obtained with the unmagnetized and magnetized NS crust given by the EDF theory [37] are shown in panels (a) and (b), respectively. The GW170817 constraint [5] is enclosed in the colored contours, and circles are the M, R values at the maximum central densities n_c.

this results agrees well with a recent conclusion by Tews and Schwenk [14].

B. Possible effects by the density dependence of the spin polarization

We note that the above results have been obtained with the spin polarization of baryons assumed to be independent of the baryon density n_b. However, the magnetic-field distribution in the NS matter is quite complex [9], and the spin polarization of baryons in a magnetar is expected to be gradually weakened with increasing baryon density. In particular, with the magnetic-field intensity diminishing to zero in the NS center [9], the spin polarization of baryons is also expected to decrease to $\Delta \approx 0$ in the central region of the magnetar. Although it is beyond the scope of the present mean-field approach to properly calculate the density profile $\Delta(n_b)$ of the spin polarization of baryons in a magnetar, we try to explore this effect by assuming three simple scenarios (A, B, and C) for the density dependence of Δ based on the magnetic-field distribution in magnetar obtained by Fujisawa and Kisaka using the Green's function relaxation method (see lower panel of Fig. 3 in Ref. [9]).

(A) The magnetic field is strongly localized in the surface region of magnetar, around the crust-core transition, and quickly decreases to $B \approx 0$ at the baryon density $n_b \approx 0.18$ fm^{-3}. We consider explicitly the spin polarization of baryons $\Delta = 0.6$, 0.8, and 1.0, which are assumed to gradually weaken to $\Delta \approx 0$ at this same density.

(B) The distribution of the magnetic-field strength is broader and covers both the crust and outer core of magnetar so that Δ decreases smoothly to zero at a larger baryon density $n_b \approx 0.35$ fm^{-3}.

(C) The magnetic-field strength is spreading to even higher baryon densities and decreasing to $B \approx 0$ at $n_b \approx 0.5$ fm^{-3}. Three considered strengths of the spin polarization of baryons are gradually weakening to $\Delta \approx 0$ at this same density.

Thus, the magnetic field in these three scenarios is completely depleted ($B = 0$) in the central region of magnetar where the baryon density n_b approaches 0.6–1 fm^{-3}. The suggested density-dependent profiles of Δ are shown together with the uniform (density independent) spin polarization of baryons (scenario D) in the upper panel of Fig. 8. The corresponding TOV results for the mass and radius of magnetar given by the density-dependent spin polarization of baryons are shown in the lower panel of Fig. 8, where the GW170817 constraint for the $R_{1.4}$ radius are plotted as the shaded contours. One can see that, when the magnetic-field strength is localized narrowly in the crust-core transition (scenario A), the mass and radius of magnetar obtained with $\Delta \lesssim 1$ are within the boundaries of the GW170817 constraint. However, with the magnetic-field strength spreading more into the outer core (scenarios A and B) the full spin polarization of baryons ($\Delta = 1$) is ruled out, and only a partial spin polarization of baryons with $\Delta \lesssim 0.8$ is possible. It is noteworthy that the EOS of partially spin-polarized NS matter with $0 \lesssim \Delta \lesssim 0.6$ gives the mass and radius of magnetar well within the GW170817 boundaries in all three scenarios (see left panel of Fig. 8).

In general, when the electromagnetic interaction between the magnetic field and NS matter is taken into account explicitly, the B-dependent contribution to the total energy density of the spin-polarized NS matter (9) is not negligible [12,13], and the discussed effects of the spin polarization of baryons to the hydrostatic NS configuration might become even more significant. Given the results of previous studies [1,2,9,12,13] on the effects of magnetic field, the total impact on the EOS of magnetar matter by magnetic field might become essential at the moderate field strength, as found in the magnetar scenario by Metzger *et al.* [8] for the blue kilonova ejecta of GW170817.

V. SUMMARY

The nonrelativistic HF approach [15] has been extended to study the spin-polarized NM using the new density-dependent CDM3Y8 version of the M3Y interaction [19], with its spin- and spin-isospin dependence adjusted to obtain the HF results close to those of the BHF calculation of the spin-polarized neutron matter [11]. Like for the nuclear (isospin) symmetry

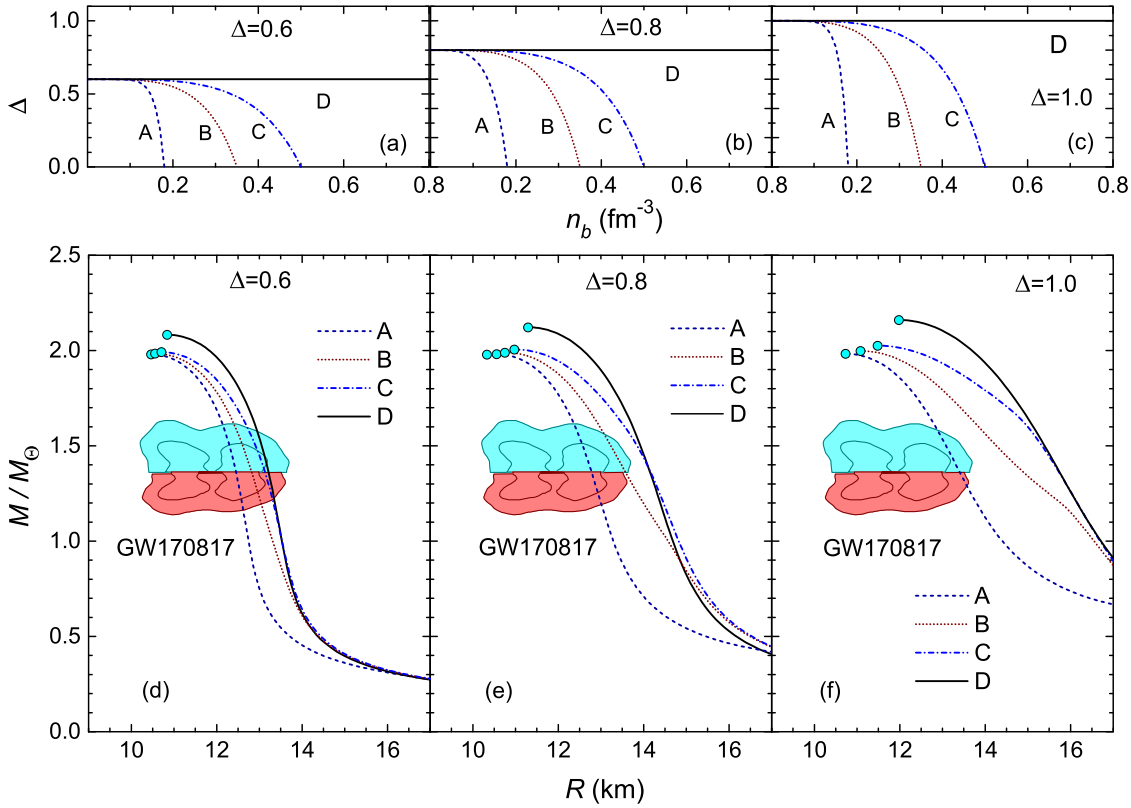

FIG. 8. Scenarios A, B, C, and D for the density-dependent spin polarization of baryons with Δ starting from 0.6, 0.8, and 1 are shown in panels (a), (b), and (c), respectively. The corresponding mass and radius of magnetar given by the EOS of the β-stable spin-polarized npeμ matter are shown in panels (d), (e), and (f), respectively. The colored contours enclose the region allowed by the GW170817 constraint [5].

energy S, the parabolic approximation was found to be valid also for the spin-symmetry energy W, so that the (repulsive) contribution to the HF energy density of NM from the spin polarization of baryons is directly proportional to Δ^2, and the EOS of NM becomes stiffer with the increasing spin polarization of baryons.

The Δ dependence of the symmetry coefficient J, the slope L, and curvature $K_{\rm sym}$ of the nuclear symmetry energy S has been investigated, and we found that the empirical ranges adopted for these quantities [35] include results of the present HF calculation with the spin polarization of baryons up to $\Delta \approx 0.8$. With the increasing Δ, the J, L, and $K_{\rm sym}$ values were found to correlate linearly with the radius $R_{1.4}$ of a NS with mass $M \approx 1.4\,M_\odot$.

The total HF energy density of the β-stable npeμ matter has been obtained at different spin polarizations of baryons, and the proton fraction $x_{\rm p}$ was found to increase strongly with increasing Δ, which in turn leads readily to a larger probability of the direct Urca process in the cooling of the magnetar.

The stiffening of the symmetry energy of the β-stable spin-polarized npeμ matter at high baryon densities has been shown to affect significantly the hydrostatic NS configuration. By subjecting the mass and radius of a NS obtained at different spin polarizations of baryons to the GW170817 constraint on the $R_{1.4}$ radius [5], we found that up to 60% of baryons might have their spins polarized during the NS merger. The same conclusion can be made when Δ is assumed to be density dependent, and the spin polarization of baryons is gradually decreasing from the surface of magnetar to zero at $n_{\rm b} \lesssim 3n_0$. These results support the magnetar origin of the blue kilonova ejecta of GW170817 suggested by Metzger *et al.* [8].

ACKNOWLEDGMENTS

The present research was supported, in part, by the National Foundation for Science and Technology Development of Vietnam (NAFOSTED Project No. 103.04-2017.317). We also thank Isaac Vidaña for his helpful communication on the BHF results of the spin-polarized neutron matter [11], and Nicolas Chamel for providing us with the EOS of the (unmagnetized and magnetized) NS crust [36,37] in the tabulated form.

[1] J. M. Lattimer and M. Prakash, Phys. Rep. **442**, 109 (2007).
[2] A. Broderick, M. Prakash, and J. M. Lattimer, Astrophys. J. **537**, 351 (2000).
[3] V. Dexheimer, B. Franzon, R. Gomes, R. Farias, S. Avancini, and S. Schramm, Phys. Lett. B **773**, 487 (2017).
[4] B. P. Abbott *et al.*, Phys. Rev. Lett. **119**, 161101 (2017).

[5] B. P. Abbott *et al.*, Phys. Rev. Lett. **121**, 161101 (2018).
[6] B. P. Abbott *et al.*, Astrophys. J. Lett. **848**, L12 (2017).
[7] P. A. Evans *et al.*, Science **358**, 1565 (2017).
[8] B. D. Metzger, T. A. Thompson, and E. Quataert, Astrophys. J. Lett. **856**, 101 (2018).
[9] K. Fujisawa and S. Kisaka, Mon. Not. R. Astron. Soc. **445**, 2777 (2014).
[10] I. Vidaña and I. Bombaci, Phys. Rev. C **66**, 045801 (2002).
[11] I. Vidaña, A. Polls, and V. Durant, Phys. Rev. C **94**, 054006 (2016).
[12] R. Aguirre, E. Bauer, and I. Vidana, Phys. Rev. C **89**, 035809 (2014).
[13] A. Isayev and J. Yang, Phys. Lett. B **707**, 163 (2012).
[14] I. Tews and A. Schwenk, Astrophys. J. Lett. **892**, 14 (2020).
[15] D. T. Loan, N. H. Tan, D. T. Khoa, and J. Margueron, Phys. Rev. C **83**, 065809 (2011).
[16] N. H. Tan, D. T. Loan, D. T. Khoa, and J. Margueron, Phys. Rev. C **93**, 035806 (2016).
[17] D. T. Khoa, G. R. Satchler, and W. von Oertzen, Phys. Rev. C **56**, 954 (1997).
[18] D. T. Khoa and G. R. Satchler, Nucl. Phys. A **668**, 3 (2000).
[19] N. Anantaraman, H. Toki, and G. Bertsch, Nucl. Phys. A **398**, 269 (1983).
[20] D. T. Khoa, W. von Oertzen, and A. Ogloblin, Nucl. Phys. A **602**, 98 (1996).
[21] A. Akmal, V. R. Pandharipande, and D. G. Ravenhall, Phys. Rev. C **58**, 1804 (1998).
[22] S. Gandolfi, A. Y. Illarionov, S. Fantoni, J. C. Miller, F. Pederiva, and K. E. Schmidt, Mon. Not. R. Astron. Soc. **404**, L35 (2010).
[23] D. T. Khoa, H. S. Than, and D. C. Cuong, Phys. Rev. C **76**, 014603 (2007).
[24] D. T. Khoa, B. M. Loc, and D. N. Thang, Eur. Phys. J. A **50**, 34 (2014).
[25] M. B. Tsang, Z. Chajecki, D. Coupland, P. Danielewicz, F. Famiano, R. Hodges, M. Kilburn, F. Lu, W. G. Lynch, J. Winkelbauer, M. Youngs, and Y. X. Zhang, Prog. Part. Nucl. Phys. **66**, 400 (2011).
[26] A. Ono, P. Danielewicz, W. A. Friedman, W. G. Lynch, and M. B. Tsang, Phys. Rev. C **68**, 051601(R) (2003).
[27] L. Trippa, G. Colò, and E. Vigezzi, Phys. Rev. C **77**, 061304(R) (2008).
[28] R. Furnstahl, Nucl. Phys. A **706**, 85 (2002).
[29] W. J. Xie and B. A. Li, Astrophys. J. Lett. **883**, 174 (2019).
[30] B. A. Li, L. W. Chen, and C. M. Ko, Phys. Rep. **464**, 113 (2008).
[31] C. J. Horowitz, E. F. Brown, Y. Kim, W. G. Lynch, R. Michaels, A. Ono, J. Piekarewicz, M. B. Tsang, and H. H. Wolter, J. Phys. G **41**, 093001 (2014).
[32] J. M. Lattimer, Nucl. Phys. A **928**, 276 (2014).
[33] U. Garg and G. Colò, Prog. Part. Nucl. Phys. **101**, 55 (2018).
[34] D. T. Khoa, W. von Oertzen, H. G. Bohlen, and S. Ohkubo, J. Phys. G **34**, R111 (2007).
[35] N. B. Zhang, B. A. Li, and J. Xu, Astrophys. J. Lett. **859**, 90 (2018).
[36] J. M. Pearson, N. Chamel, A. Y. Potekhin, A. F. Fantina, C. Ducoin, A. K. Dutta, and S. Goriely, Mon. Not. R. Astron. Soc. **481**, 2994 (2018).
[37] Y. D. Mutafchieva, N. Chamel, Z. K. Stoyanov, J. M. Pearson, and L. M. Mihailov, Phys. Rev. C **99**, 055805 (2019).
[38] F. Douchin and P. Haensel, Astron. Astrophys. **380**, 151 (2001).
[39] P. B. Demorest, T. Pennucci, S. M. Ransom, M. S. E. Roberts, and J. W. T. Hessels, Nature (London) **467**, 1081 (2010).
[40] Z. Arzoumanian *et al.*, Astrophys. J., Suppl. Ser. **235**, 37 (2018).
[41] J. Antoniadis *et al.*, Science **340**, 1233232 (2013).
[42] H. T. Cromartie, E. Fonseca, S. M. Ransom *et al.*, Nat. Astron. **4**, 72 (2020).
[43] C. Y. Tsang, M. B. Tsang, P. Danielewicz, F. J. Fattoyev, and W. G. Lynch, Phys. Lett. B **796**, 1 (2019).